

Effect of Acute Pancreatitis on Lung Structure of Adult Male Albino Rats and Role of Allopurinol Administration

Maha A. Abdallah and Dalia A. Mohamed

Histology and Cell Biology Department, Faculty of Medicine, Zagazig University
maha18770@gmail.com

Abstract: **Introduction:** Acute pancreatitis not only affects the pancreas, but also has many systemic manifestations. Acute lung injury is one of its most common and serious complications. **Aim of work:** This work aimed to study the effect of experimentally induced pancreatitis on the lung structure of adult male albino rats and the role of allopurinol administration. **Materials & methods:** Thirty adult male albino rats were equally divided into three groups; control (I), main pancreatic duct ligated (II) and allopurinol treated main pancreatic duct ligated (III). After pancreatic duct ligation, rats of all groups were left free in their cages for four successive days. Rats of group III were injected intraperitoneally by 200 mg allopurinol per kg body weight every 12 hours during these four days. By the end of fourth day, blood samples of all rats were collected for the evaluation of serum amylase. Rats' lungs were dissected out and processed for light and electron microscope examination. Area percentages of collagen fibers and inducible nitric oxide synthase; iNOS as well as serum amylase level were estimated and statistically analyzed. **Results:** Most of the lung alveoli of group II were markedly collapsed. Others were filled by homogenous acidophilic material and extravasated blood. They were separated by thickened septa containing congested blood vessels, many inflammatory cells and moderate aggregations of collagen fibers. Some pneumocytes type I had heterochromatic shrunken nuclei. Pneumocytes type II cytoplasm was distended with variable sized lamellar bodies with marked loss of their lamellar arrangement. Numerous alveolar macrophages in the alveolar cavities and extensive neutrophilic infiltration within the interalveolar septum were observed. Many strong positive iNOS immune reactive cells were observed. In group III, relatively narrow alveoli were observed. Few of them contained homogenous acidophilic material. The interalveolar septa were thin in most areas and moderately thickened in other ones containing thin collagen fibers and inflammatory cells. The alveolar wall was lined by pneumocytes type I and few pneumocytes type II. Pneumocyte type I had irregular euchromatic nuclei surrounded by thin rim of cytoplasm. Pneumocytes type II cytoplasm contained lamellar bodies. Some of these bodies retained their lamellar arrangement while others were disorganized. Few strong positive iNOS immune reactive cells were observed. Estimated and analyzed data for collagen fibers, iNOS area % and serum amylase level confirmed the results. **Conclusion:** Acute pancreatitis led to structural alterations in lung parenchyma and these changes were markedly reduced by allopurinol injection at the early stage of acute pancreatitis. So, allopurinol administration may be beneficial in prevention of acute lung injury associated with pancreatitis.

[Maha A. Abdallah and Dalia A. Mohamed. **Effect of Acute Pancreatitis on Lung Structure of Adult Male Albino Rats and Role of Allopurinol Administration.** *Life Sci J* 2014;11(3):82-93]. (ISSN:1097-8135). <http://www.lifesciencesite.com>. 12

Key words: Acute pancreatitis – lung – Allopurinol – pneumocytes - ultrastructure

1. Introduction

Acute pancreatitis (AP) is an acute inflammatory disease of the pancreas. It is generally associated with severe upper abdominal pain and is diagnosed mainly by concomitant increase in the serum amylase and lipase [1-3]. AP has high morbidity and mortality rate reaching 20-30% in severe cases [4]. The mortality rate can increase up to 50 % as a result of induction of systemic inflammatory response syndrome during early stages that finally cause multisystem organ failure [5,6].

Pulmonary complications are the most frequent and potentially serious systemic complications of AP. They include hypoxia, acute respiratory distress syndrome, atelectasis and pleural effusion. Although, hypoxemia may occur without any radiological

abnormalities in 75% of cases, it is considered a direct cause of mortality [7].

The most common causes of AP are gall bladder stone disease, alcohol ingestion and drugs as antihypertensives, calcium channel blockers, proton pump inhibitors and H₂ blockers. Clinical studies suggested that the onset of gall stone-induced pancreatitis requires migration of the offending stones through the biliary tract and its impaction at the duodenal papilla [3,8,9]. Severe acute pancreatitis usually occurs if gall stones are lodged in the common channel that normally formed from union of common bile duct and pancreatic duct. Obstruction of a common channel might lead to reflux of pancreatic juice into the common bile duct. The mixing of bile

and pancreatic juice may lead to formation of a substance that is highly toxic to the pancreas [10].

Allopurinol is a commonly prescribed drug used to treat gout and certain types of kidney stones. Also, it prevents increased uric acid levels in patients receiving cancer chemotherapy not only by blocking uric acid production but also by inhibition of xanthine oxidase enzyme. This enzyme is claimed to have a role in the pathogenesis of AP. It is activated in early stage and generates reactive oxygen species that subsequently induce oxidative damage to DNA, RNA and proteins within the cells [11-14]. So, this research aimed to study the effect of experimentally induced pancreatitis on the lung structure of adult male albino rats and the role of allopurinol administration.

2. Materials & Methods

Thirty healthy adult male albino rats (4-6 months) weighing 180-200 g were used in this study. They were housed in stainless-steel cages and were maintained in room temperature at 23°C. They were allowed water *ad libitum* and were fed a standard diet. They were equally divided into three groups: a control (I), main pancreatic duct ligated (II) and Allopurinol treated main pancreatic duct ligated (III). The control group is further subdivided into two subgroups; rats without any surgical procedure; non-operated (Ia) and sham operated rats (Ib).

Rats of the subgroup Ib, groups II&III were anesthetized with 50 mg sodium pentobarbital per kg body weight intraperitoneally. Under sterile condition, a midline abdominal incision was made and the pancreas was exposed. In both groups (II & III), ligation of the main pancreatic duct was done just adjacent to its entrance into the duodenum with 6-0 silk thread. In sham operated subgroup (Ib), the same procedure was performed without ligation of the main pancreatic duct. The abdominal incision was sutured. Then, rats of all groups were left free within their cages for four successive days [15]. After 2 hours of pancreatic duct ligation, rats of group III received 200 mg allopurinol per kilogram body weight intraperitoneally every 12 hours during these four days [12]. Allopurinol was manufactured by Galxosmithkline S.A.E. Elsalam City, Cairo.

At the end of the fourth day after duct ligation, blood samples from the rats' tails of all groups were collected for evaluation of serum amylase level; an indicator of pancreatitis [12]. Then, all rats were anesthetized with 50 mg sodium pentobarbital per kg body weight intraperitoneally and then intracardiac perfusion was done by 2.5% glutaraldehyde buffered with 0.1 M phosphate buffer at pH 7.4 for partial fixation of the lungs. Then, the left lungs of rats in all groups were dissected out carefully and were processed for light and electron microscopic

examinations. Specimens for light microscope examination were fixed in 10% neutral formal saline for 24 hours and were processed to prepare 5 µm thick paraffin sections for Haematoxylin & Eosin, Mallory Trichrome and immunohistochemical stains for detection of inducible nitric oxide synthase; iNOS [16].

Immunostaining was performed using avidin-biotin peroxidase technique to detect the expression of iNOS in lung tissue. Sections underwent deparaffinization and hydration. They were treated with 0.01M citrate buffer (pH 6.0) for 10 minutes to unmask antigen. Then, they were incubated in 0.3% H₂O₂ for 30 minutes to abolish endogenous peroxidase activity before blocking with 5% horse serum for 1-2 hrs. Slides were incubated with rabbit polyclonal anti-iNOS (Abcam, at dilution 1:100) at 4°C for 18-20 hrs, then washed and incubated with biotinylated secondary antibodies followed with avidin-biotin complex. Finally, sections were developed with 0.05% diaminobenzidine slides, were counter stained with Meyer's hematoxylin, dehydrated, cleared and mounted. iNOS positive cells exhibited brown colored cytoplasm and blue stained nuclei [17].

Specimens for electron microscope examination were immediately fixed in the same perfusion fixative (2.5 % glutaraldehyde) for 2 hrs and postfixed in 1% osmium tetroxide buffered with 0.1 M phosphate buffer at pH 7.4 for 1 h. Then, they were dehydrated in ascending grades of ethyl alcohol and embedded in epoxy resin to prepare semithin sections and ultrathin sections using a Leica ultracut (UCT) (Glienicker, Berlin, Germany). Semithin sections (1 µm thick) were stained with 1% toluidine blue for light microscope examination [16]. Ultrathin sections were stained with uranyl acetate and lead citrate [18]. They were examined with a JEOL JEM 1010 transmission electron microscope (Japan) in the Electron Microscope Research Laboratory (EMRL) of the Histology and Cell Biology Department, Faculty of Medicine, Zagazig University (Egypt).

Morphometric study:

The image analyzer computer system Leica Qwin 500, UK in the Histology Department, Faculty of Medicine, Cairo University, was used to count the mean area percentage for iNOS immunoreactions using the immunostained lung sections. Ten non-overlapping high-power fields (X400) from each slide of all animals of each group were used and the positive immunoreactive cells were counted. Also the collagen area percentage was detected in Mallory stained sections by the same way.

Statistical analysis

Data for all groups were expressed as mean ± standard deviation (X±SD). The data obtained from

the image analyzer were subjected to SPSS programme version 17. Statistical significant difference was determined by one way analysis of variance (ANOVA). The probability values (P) < 0.05 < 0.001 and > 0.05 were considered significant, highly significant and non-significant respectively.

3.Results

I- Histological result

Light microscope examination of sections in the lung of the control adult male albino rats (Ia and Ib) showed that the lung parenchyma had bronchioles, alveolar ducts, alveolar sacs and clusters of alveoli that were separated by thin interalveolar septum. Bronchiolar wall was lined by pseudostratified epithelium surrounded by circular smooth muscle fibers (Figs. 1&2). The alveoli were lined by simple epithelium composed of two cell types; flattened cells with flattened nuclei; pneumocytes type I and cuboidal cells with irregular nuclei and vacuolated cytoplasm; pneumocytes type II (Fig. 3). Thin collagen fibers were observed in the interalveolar septa (Fig. 4). Few strong positive iNOS immune reactive cells were observed (Fig. 5).

Electron microscope examination of the ultrathin sections of the same group showed that pneumocytes type I had euchromatic nuclei surrounded by thin rim of cytoplasm (Fig. 6). Pneumocytes type II cytoplasm contained numerous lamellar bodies and mitochondria. Short apical microvilli were observed on their free surfaces (Fig. 7). Alveolar macrophages had irregular nuclei within peripheral rim of heterochromatin. Their cytoplasm contained electron dense bodies (Fig. 8).

Light microscope examination of the sections in rats' lung of group II showed that most of the lung alveoli were markedly collapsed (Fig. 9). Numerous alveoli were filled by homogenous acidophilic material and extravasated blood (Fig. 10). The alveoli were separated by thickened interalveolar septa containing congested blood vessels and many inflammatory cells (Fig. 11) in comparison with that observed in the control group. The alveolar epithelial lining comprised numerous pneumocytes type II distended with many vacuoles (Fig. 12) Moderate

aggregations of collagen fibers were detected in the thickened interalveolar septa (Fig. 13). Many strong positive iNOS immune reactive cells were observed (Fig. 14).

Electron microscope examination of the ultrathin sections of the lung of the same group showed that some of the pneumocytes type I had irregular euchromatic nuclei with peripheral heterochromatin and thin rim of cytoplasm. Others had heterochromatic shrunken nuclei. Fibroblasts with irregular nuclei, mitochondria, intra and extra-cellular collagen fibers were observed within the alveolar septa (Fig. 15). Pneumocytes type II cytoplasm was distended by variable sized lamellar bodies with marked loss of their lamellar arrangement (Fig. 16). Numerous alveolar macrophages were frequently seen within the alveolar cavities (Fig. 17). Extensive neutrophilic infiltration was observed within the interalveolar septa (Fig. 18).

Light microscope examination of the sections in rats' lung of group III revealed relatively narrow alveoli in comparison with that noticed in group I. Few of them contained homogenous acidophilic material (Fig. 19). The interalveolar septa were thin in most areas and moderately thickened in other ones containing inflammatory cells (Fig. 20). The alveolar wall was lined by pneumocytes type I and few pneumocytes type II (Fig. 21) in comparison with group II. Most of the interalveolar septa exhibited thin collagen fibers (Fig. 22). Few strong positive iNOS immune reactive cells were observed (Fig. 23).

Electron microscope examination of the ultrathin sections of the same group revealed that pneumocytes type I had irregular euchromatic nuclei surrounded by thin rim of cytoplasm (Fig. 24). Pneumocytes type II cytoplasm contained lamellar bodies and mitochondria. Some of these bodies retained their lamellar arrangement while others were disorganized (Fig. 25).

II- Biochemical results:

The present study revealed significant elevation of the serum amylase level in rats of groups II&III in comparison to those of control rats. The elevated level of serum amylase is higher in group II than group III.

Table (1): The mean of serum amylase level

	$\bar{X} \pm SD$ (Range)	t	P
Group I	322±46		
Group II	2012±254	20.7	*0.001
Group III	1221±105	24.8	*0.0003

$F = 168.38$ * $p < 0.001$

III-Morphometrical and statistical results:

Table (2):The mean area percentage of the collagen fibers in different groups.

	X±SD (Range)	t	P
Group I	6.98±1.6 (5.46-9.5)		
Group II	16.9±6.0 (8.62-23.55)	3.55	0.007*
Group III	12.79±4.9 (5.0-17.17)	2.5	0.03*

F = 4.45

P= 0.018*

Table (3): The mean area percentage of iNOS immunoreaction in different groups.

	X±SD (Range)	t	P
Group I	20.5±3.0 (15.8-23.7)		
Group II	39.5±5.73 (33.66-48.21)	6.56	<0.001**
Group III	36.4±4.9 (26.6-46.2)	7.59	<0.001**

F = 17.64

P<0.001*

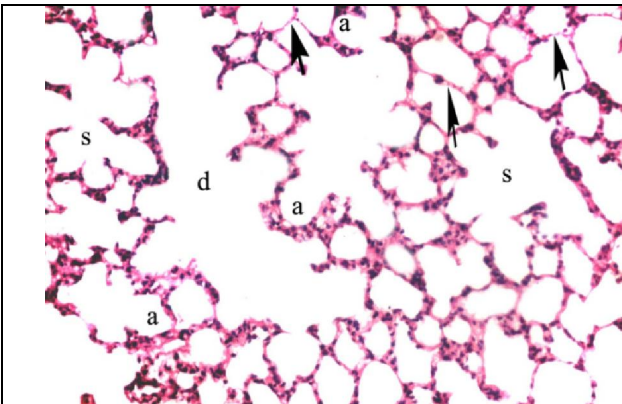


Figure (1): A photomicrograph of a section in the control lung showing alveolar duct (d), alveolar sacs (s) and alveoli (a) separated by thin interalveolar septa (arrows). (H&E X100).

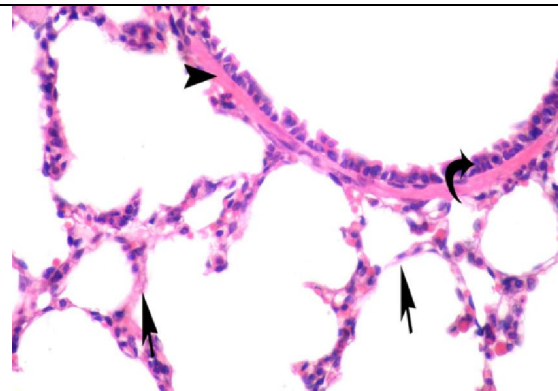


Figure (2): A photomicrograph of a section in the control lung showing a bronchiole lined by pseudostratified epithelium (curved arrow) surrounded by circular smooth muscle fibers (arrow head). Thin alveolar septa (arrows) are noticed. (H&EX400).

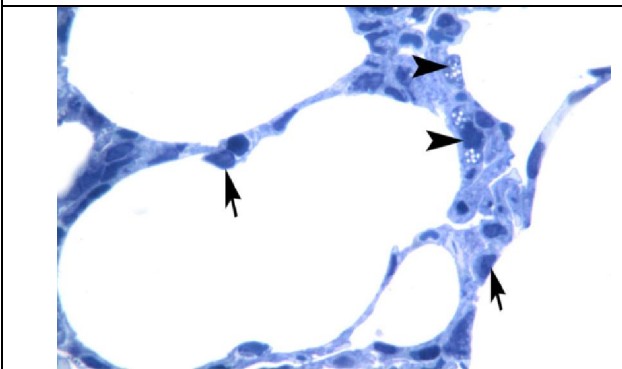


Figure (3): A photomicrograph of a semithin section (1µm thick) in the control lung showing the simple alveolar epithelium with two cell types: pneumocytes type I (arrows) and pneumocytes type II (arrow heads). (Toluidine blue: X 1000).

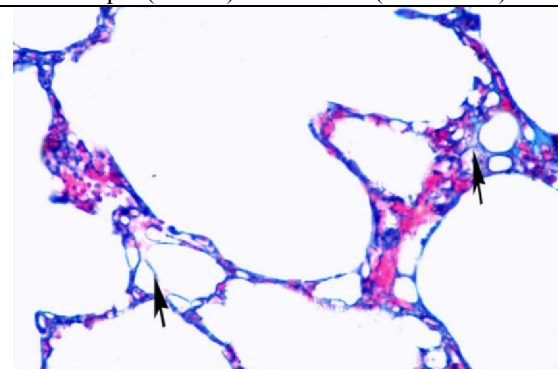


Figure (4): A photomicrograph of a section in the control lung showing thin collagen fibers (arrows) in the interalveolar septa. (Mallory trichrome X400).

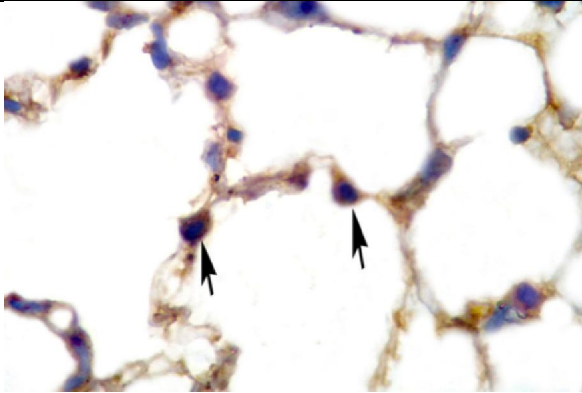


Figure (5): A photomicrograph of a section in the control lung showing few strong positive iNOS immune reactive cells (arrows). (Avidin biotin peroxidase system X 1000).

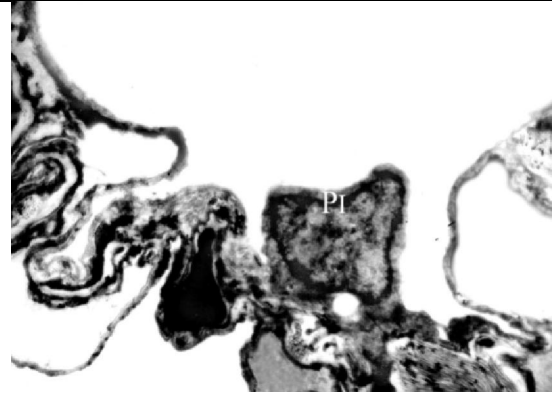


Figure (6): An electron micrograph from the control lung showing that the pneumocyte type I (PI) has euchromatic nucleus surrounded by a thin rim of cytoplasm. (Mic. Mag. X 4000).

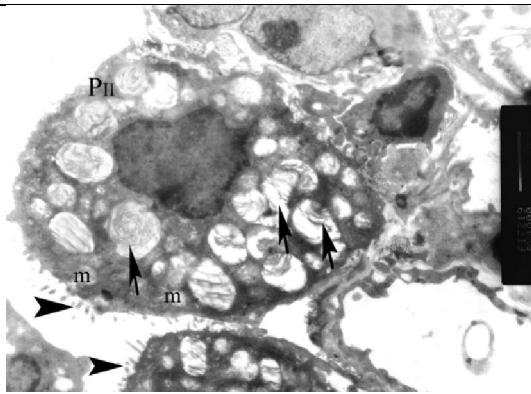


Figure (7): An electron micrograph from the control lung showing that the pneumocytes type II (PII) cytoplasm contains numerous lamellar bodies (arrows) and mitochondria (m). Short apical microvilli (arrow heads) are observed on their free surfaces. (Mic. Mag. X 4000).

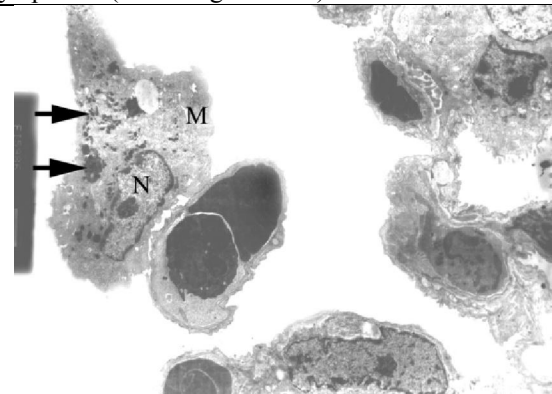


Figure (8): An electron micrograph from the control lung showing that an alveolar macrophage (M) has irregular nucleus (N) with heterochromatin. Its cytoplasm contains electron dense bodies (arrows). (Mic. Mag. X 4000).

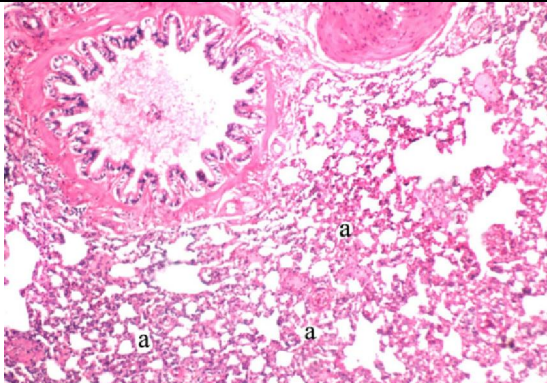


Figure (9): A photomicrograph of a section in the rats' lung of group II showing that most of the alveoli (a) are markedly collapsed. (H&E X100).

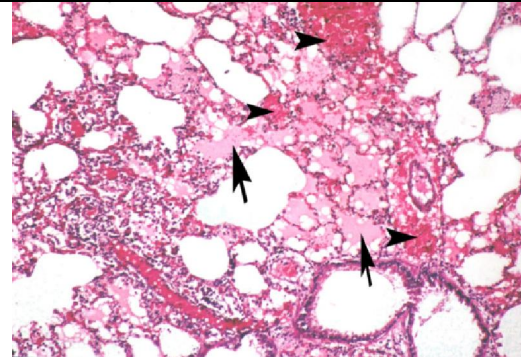


Figure (10): A photomicrograph of a section in the rats' lung of group II showing that numerous alveoli are filled by homogenous acidophilic material (arrows) and extravasated blood (arrow heads). (H&E X200).

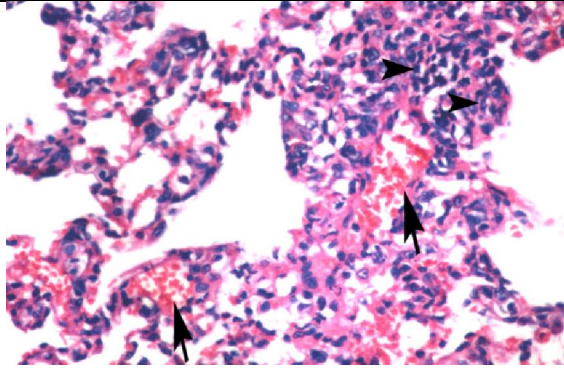


Figure (11): A photomicrograph of a section in the rats' lung of group II showing thickened interalveolar septa containing congested blood vessels (arrows) and many inflammatory cells (arrow heads) in comparison with that observed in fig. 2. (H&E X400).

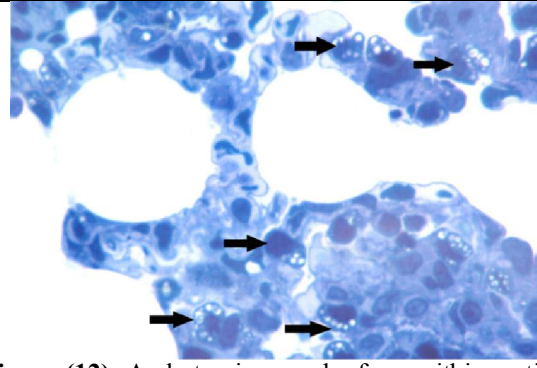


Figure (12): A photomicrograph of a semithin section (1µm thick) in the rats' lung of group II showing numerous pneumocytes type II (arrows) distended with many vacuoles. (Toluidine blue: X1000).

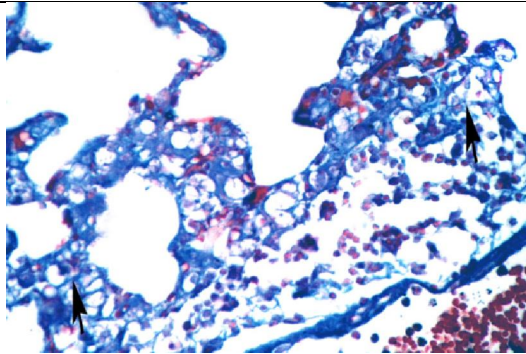


Figure (13): A photomicrograph of a section in the rats' lung of group II showing moderate aggregations of collagen fibers (arrows) in the thickened interalveolar septa. (Mallory trichrome X400).

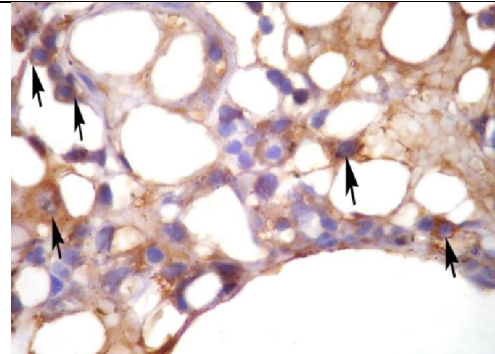


Figure (14): A photomicrograph of a section in the rats' lung of group II showing many strong positive iNOS immune reactive cells (arrows). (Avidin biotin peroxidase system X 1000).

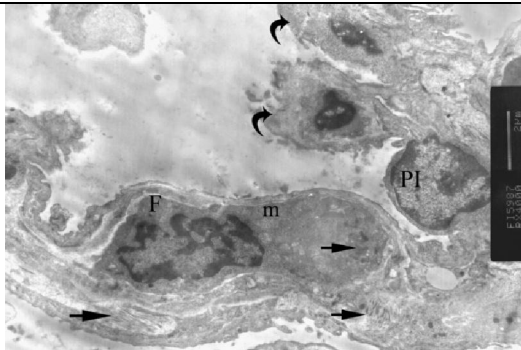


Figure (15): An electron micrograph from the rats' lung of group II showing pneumocyte type I (PI) with irregular euchromatic nucleus and peripheral heterochromatin surrounded by thin rim of cytoplasm. Others (curved arrows) have heterochromatic shrunken nuclei. A fibroblast (F) with irregular nucleus, mitochondria (m), intra and extra-cellular collagen fibers (arrows) is observed within the alveolar septum. Notice the homogenous moderately electron dense material in the alveolar lumen (Mic. Mag. X 4000).

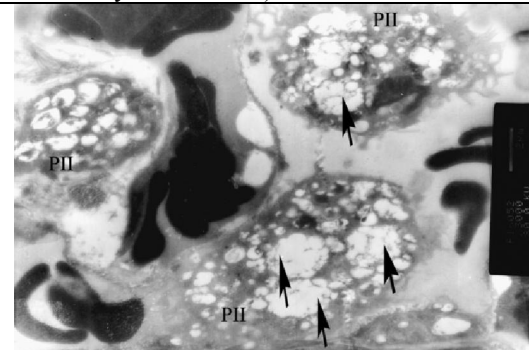


Figure (16): An electron micrograph from the rats' lung of group II showing that the pneumocytes type II (PII) cytoplasm is distended by variable sized lamellar bodies (arrows) with marked loss of their lamellar arrangement. (Mic. Mag. X 4000).

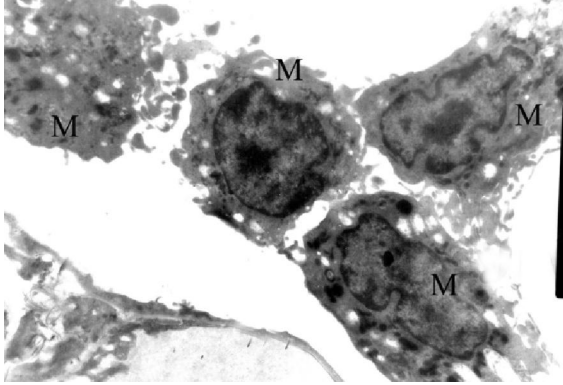


Figure (17): An electron micrograph from the rats' lung of group II showing numerous alveolar macrophages (M) within the alveolar cavities. (Mic. Mag. X 4000).

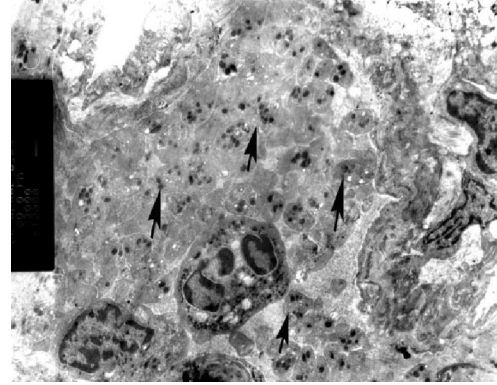


Figure (18): An electron micrograph from the rats' lung of group II showing extensive neutrophilic infiltration (arrows) within the interalveolar septum. (Mic.Mag.X3000).

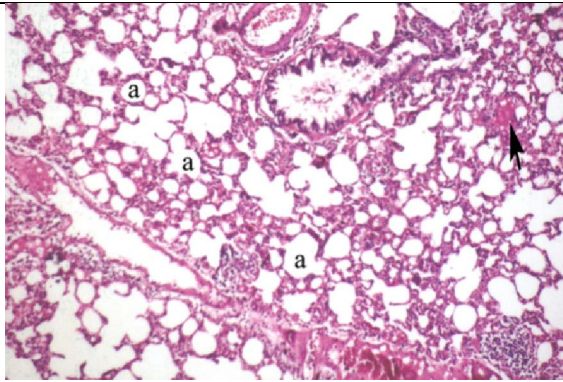


Figure (19): A photomicrograph of a section in the rats' lung of group III showing relatively narrow alveoli (a) in comparison with fig. 1. Few of them contain homogenous acidophilic material (arrow). (H&E X100).

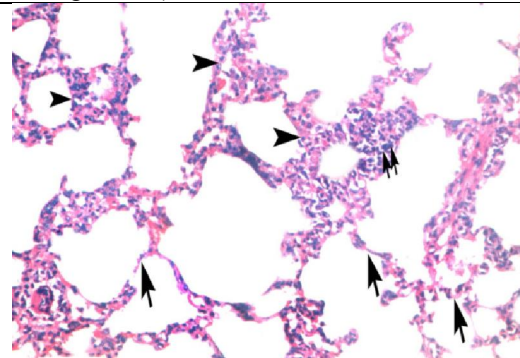


Figure (20): A photomicrograph of a section in the rats' lung of group III showing thin interalveolar septa (arrows) in most areas. Moderately thickened septa (arrow heads) are also noticed containing inflammatory cells (double arrow). (H&E X 400).

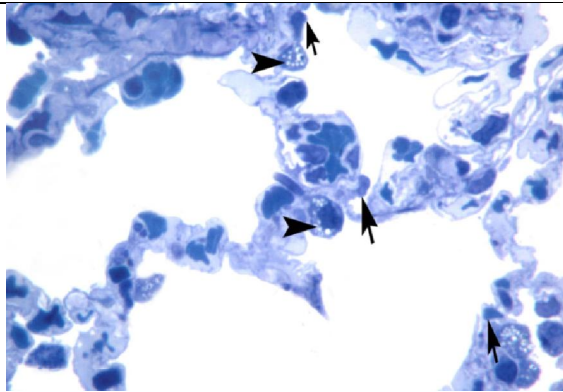


Figure (21): A photomicrograph of a semithin section (1µm thick) in the rats' lung of group III showing that the alveolar wall is lined by pneumocytes type I (arrows) and few pneumocytes type II (arrow heads) in comparison with fig.12. (Toluidine blue: X1000).

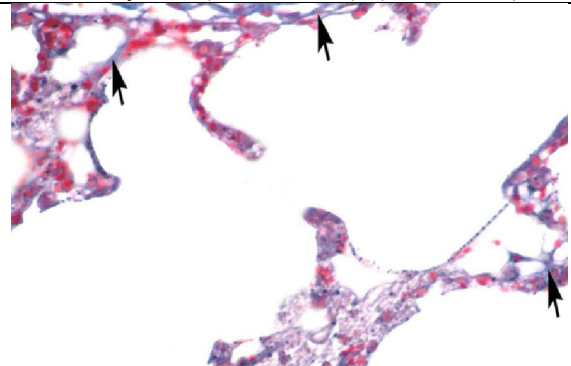


Figure (22): A photomicrograph of a section in the rats' lung of group III showing thin collagen fibers (arrows) in most of the interalveolar septa. (Mallory trichrome X400).

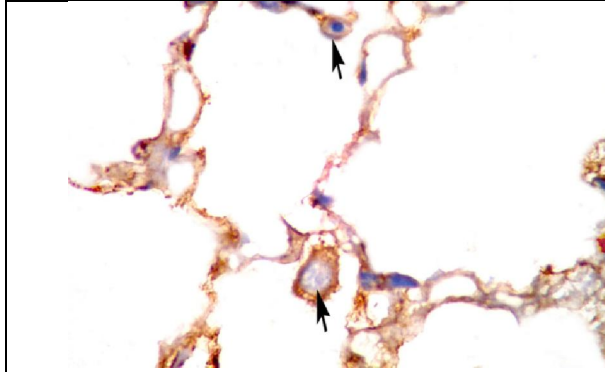


Figure (23): A photomicrograph of a section in the rats' lung of group III showing few strong positive iNOS immune reactive cells (arrows). (Avidin biotin peroxidase system X 1000).

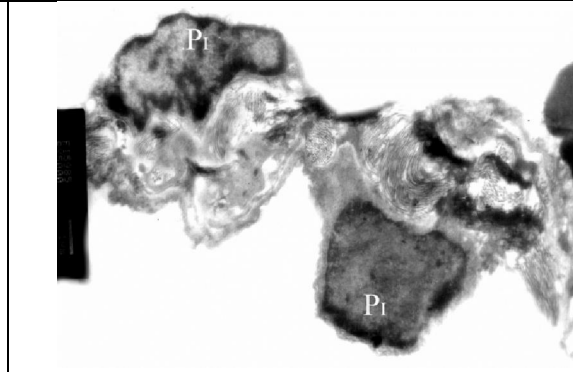


Figure (24): An electron micrograph from the rats' lung of group III showing pneumocytes type I (PI) with irregular euchromatic nucleus surrounded by thin rim of cytoplasm. (Mic. Mag. X 4000).

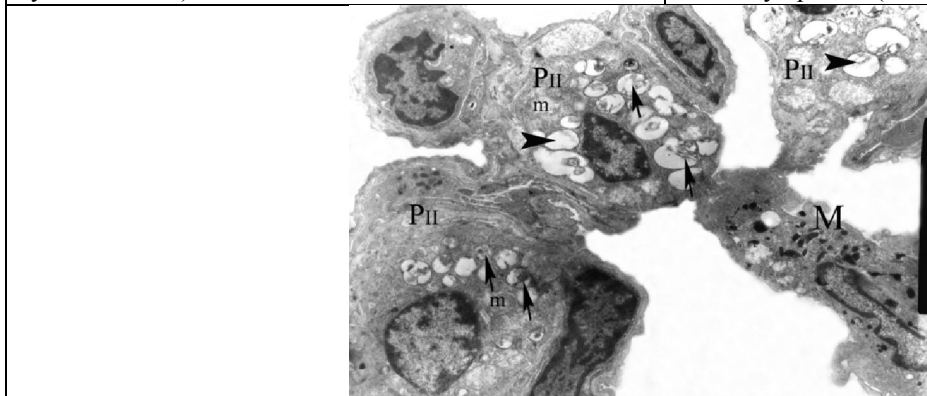


Figure (25): An electron micrograph from the rats' lung of group III showing that pneumocytes type II (PII) cytoplasm contains lamellar bodies and mitochondria (m). Some of these bodies retain their lamellar arrangement (arrows) while others are disorganized (arrow heads). Intra-alveolar macrophage (M) with irregular nucleus is also observed. (Mic. Mag. X 4000).

4. Discussion

Acute pancreatitis (AP) is an autodigestive process in which digestive enzymes in the exocrine pancreas become activated and released within the gland instead of being secreted into the gastrointestinal tract. Subsequently, these enzymes induce acinar cells injury and hyperamylasemia. The consequences of this inflammatory process not only affect the pancreas, but also have many systemic manifestations. Pulmonary complications frequently occur secondary to AP and are a common cause of morbidity and mortality [3,19].

The present study revealed significant elevation of the serum amylase level in rats of groups II&III in comparison to those of control group. The elevated level of serum amylase is higher in group II than group III. It was documented [20] that amylase is a sensitive index reflecting pancreatitis. Additionally [21], amylase content was positively correlated with the activation of nuclear factor kappa-light-chain-enhancer of activated B cells (NF- κ B); a protein

complex that controls transcription of DNA. Disturbance of NF- κ B regulation has been linked to cancer, inflammatory and improper immune development. So, amylase can induce pancreatic injury directly or by multiple organs injury through inflammatory response mediated by the activation of NF- κ B.

In main duct ligated rats, most of the lung alveoli were markedly collapsed. Numerous alveoli were filled by homogenous acidophilic material and extravasated blood. Some researchers [7,22] reported that AP is usually associated with high level of pancreatic enzymes as trypsin that subsequently activate pulmonary phospholipase A2 (PLA2). PLA2 has the ability to remove fatty acids from phospholipids which is considered as one of the main component of surfactant. Marked reduction of surfactant production within the alveoli is usually responsible for alveolar collapse. In addition, trypsin causes damage to the pulmonary vasculature and increases endothelial permeability leading to lung

edema. Subsequently[23], the lungs become edematous and congested leading to collapse of the smaller airways with decreased lung compliance and respiratory failure.

The alveoli of main duct ligated rats were separated by thickened interalveolar septa containing many inflammatory cells. Extensive neutrophilic infiltration was observed within the interalveolar septum. It was reported [24,25] that lung injury secondary to AP may be further aggravated by the recruitment of neutrophils in lung capillaries. Adhesion molecules such as P-selectin and intracellular adhesion molecule-1 (ICAM-1) mediate the neutrophil-endothelial cell interactions. Once neutrophils adhere to the pulmonary endothelium, they release various substances as proteases and oxygen radicals that are thought to be more damaging to the lungs than the circulating pancreatic enzymes. Some scientists [19] recorded a transient drop in the number of circulating neutrophils associated with an increase in the number of migrating neutrophils in the lungs. Neutrophils produce proteases enzymewhich have the capability to fragment the underlying fibronectin matrix. These fibronectin fragments act as a potent chemotactic signal for other circulating mononuclear cells. Others attributed[7] neutrophil infiltration to the presence of platelet activating factor (PAF); a pro-inflammatory phospholipid alters microvascular permeability and subsequently promotes activation and migration of inflammatory cells especially polymorphonuclear cells (PMNs). Administration of the PAF degrading enzyme (PAF acetylhydrolase) prevents the development of pancreatitis-associated lung injury. Other scientists [26] stated that induction of AP was associated with a significant increase in pancreatic and lung myeloperoxidase (MPO) activity, indicating that neutrophils were sequestered in both organs. Over the past decade, various researchers [27] have suggested the important role of various pro-inflammatory cytokines in both local and systemic complications of AP. In this concept, interleukin-1 β (IL-1 β) is believed to enhance local tissue destruction and distant organ complications. So, it has been claimed [28,29] that the systemic levels of IL-1 β can be used as a marker for predicting the severity of AP.

In this search, rats' lung of group II showed many congested blood vessels within the interalveolar septa. Extravasated blood was observed within the alveoli. Some investigators [22, 30] correlated the previous observation either to neuropeptide substance P which is released from the nerve endings or the sequel of endothelial cell damage in the alveolar capillaries. Substance P can mediate abnormal vascular permeability during acute inflammation and erythrocytes extravasation through the gaps between

the damaged endothelial cells. This hypothesis is supported by the finding that the concentration of substance P was twofold higher in the pulmonary edema fluid of patients with acute respiratory distress syndrome.

In this work, the alveoli of duct ligated rats contained some pneumocytes type I cells had irregular euchromatic nuclei with peripheral heterochromatin and thin rim of cytoplasm. Others had heterochromatic shrunken nuclei. Some scientists reported [31,32] that AP led to widespread apoptosis, necrosis and also exfoliation of type I pneumocytes. They attributed this to excess production of oxygen-derived free radicals (OFRs) from activated neutrophils. Accumulation of OFRs, initiate a series of oxidative stresses that subsequently induce lipid peroxidation not only in the cell membranes but also in cell organelles' membranes. Oxidative stress results in lesions of cells, mitochondria and more lysosomal enzymes production. These events evoke further destruction of vascular endothelial cells and subsequent increase the permeability of capillaries. Others claimed [33] that tumor necrosis factor- α (TNF- α), mainly produced by mononuclear cells, is not only capable of directly killing cells but is also capable of promoting the production of other cytokines. However, it was explained [22] that high level of phospholipase A2 secondary to AP may induce apoptosis through transformation of lecithin that normally present in cell membranes into more toxic compound lysolecithin.

In group II, the alveolar epithelial lining comprised numerous pneumocytes type II distended with many vacuoles. Ultrastructurally, their cytoplasm contained variable sized lamellar bodies with marked loss of their lamellar arrangement. It was stated [22,34,35] that pneumocytetype II are responsible for surfactant synthesis that control the volume and composition of the epithelial lining fluid. These cells may also proliferate and differentiate into type I alveolar epithelial cells after lung injury to maintain the integrity of the alveolar walls. They increased and migrated closer and/or through the alveolar type I epithelial cells. Additionally [32, 36], lamellar bodies not only decreased in number but also progressively vacuolated that subsequently may affect the surfactant production and secretion. Some scientists [37] classified the acute lung injury into two phases; an initial exudative phase in which a diffuse alveolar damage, pneumocyte type I necrosis and influx of inflammatory cells. This is followed secondly by proliferative phase which include pneumocytetype II hyperplasia and fibroblast proliferation.

In this study, moderate aggregations of collagen fibers were detected in the thickened interalveolar septa of main duct ligated group. Fibroblasts with irregular nuclei, mitochondria, intra and extra-cellular

collagen fibers were observed within the alveolar septa. Statistically, the mean area percentage of collagen fibers immune reaction was significantly increased. Previous studies [38] had shown that fibroblasts are the major cells responsible for the synthesis of matrix elements in connective tissue and constitute 35–40% of the cell in the interstitium of the lung. Although fibroblasts remain largely quiescent under normal conditions, they are activated to proliferate and synthesize various cytokines during inflammation, suggesting that they may contribute to the pathophysiology of certain lung diseases. In addition to collagen fibers deposition, it was found [39] that fibroblasts can release soluble chemotactic factors for both neutrophils and monocytes migration. Furthermore [30], tissue hypoxia usually activate alveolar macrophages to release mitogenic factors that subsequently stimulate interstitial fibroblasts to deposit excess collagen. Others [40] reported that injured lung is believed to go through three phases: exudative, proliferative and fibrotic. During proliferative phase, pneumocyte type II proliferates to reline the denuded basement membrane. Concomitantly, fibroblasts become pronounced to deposit collagen fibers in the interstitium around the injured alveoli. The fibrotic phase was characterized by excessive aggregation of collagen fibers type I around alveolar duct.

In the current study, lungs of group II showed numerous alveolar macrophages were frequently seen within the alveolar cavities. Some investigators [7,41,42] previously noted that alveolar macrophages were activated by phospholipase A2; mainly secreted by pancreas in AP. Activated macrophages produced a large amount of TNF- α and nitric oxides (NO) that contributed to lung injury. They play an important role in chemotaxis of further leucocytes. They also mediate endothelial injury as well as increase microvascular permeability resulting in lung injury. In contrast, other researchers [43] classified lung macrophages into alveolar and interstitial ones. Both type play distinct roles in the acute lung injury associated with AP. Alveolar macrophages promote an early inflammatory response, whereas interstitial ones appear to have a protective role to resolve the inflammation.

In this work, lung tissue of group (II) showed many strong positive iNOS immune reactive cells were observed. Statistically, the mean area percentage of iNOS immunoreaction was significantly increased. Early studies [44] documented normal expression of the enzyme; inducible nitric oxide synthase; iNOS in human lung cells, including epithelial, septal macrophages, vascular and inflammatory cells. It was reported [45] that immunoreactivity for iNOS is mainly localized in type 2 pneumocytes. Excessive production of NO via iNOS can cause adverse effects

in lung tissue by reactions with superoxide anion leading to development of reactive nitrogen species. Other scientists [21,37] correlated the expression level of iNOS with the activation of NF- κ B in lung tissue. NF- κ B is a central transcription factor that controls the expression of multiple inflammatory genes, such as TNF- α , IL-6, IL-8 and inducible nitric oxide synthase (iNOS). Overexpression of these factors can cause damage to pancreatic and extra-pancreatic tissues. A correlation between NF- κ B activation, serum amylase, reactive oxygen species (ROS) levels, pancreatic and pulmonary tissue damage has been implicated in the pathogenesis of AP. Inhibition of NF- κ B activation prevent pancreatic damage and reactive oxygen species (ROS) production.

In this search, lungs of group III revealed relatively narrow alveoli. Few of them contained homogenous acidophilic material. They had thin interalveolar septa in most areas and moderately thickened ones containing inflammatory cells and thin collagen fibers. The alveolar wall was lined by pneumocytes type I and few pneumocytes type II in comparison with group II. Pneumocytes type I had irregular euchromatic nuclei surrounded by thin rim of cytoplasm. Pneumocytes type II cytoplasm contained lamellar bodies and mitochondria. Some of these bodies retained their lamellar arrangement while others were disorganized. Few positive iNOS immune reactive cells were observed. It was reported [46,47] that allopurinol is rapidly oxidized by xanthine oxidase enzyme (XO) to its active metabolite oxypurinol. Both of them can improve lung injury not only through inhibition of neutrophil infiltration within the lung but also through antibacterial activity. Other scientists [48], claimed that allopurinol had an ability to block p38 expression that might have an active role in the induction of apoptosis, in response to various environmental stimuli. It was added [12,47] that allopurinol has the ability to inhibit reactive oxygen species through inhibition of XO and subsequently oxidative stress. Additionally, they can actually reduce XO expression. Other researchers reported [49] that allopurinol treatment could prevent the generation of ROS and also reduce serum amylase concentration. So, allopurinol ameliorates pancreatic edema, necrosis and inflammation.

Conclusion:

Acute pancreatitis led to structural alterations in lung parenchyma and these changes were markedly reduced by allopurinol injection at the early stage of acute pancreatitis. So, allopurinol administration may be beneficial in prevention of acute lung injury associated with pancreatitis.

Corresponding author**Maha A. Abdallah**

Histology and Cell Biology Department, Faculty of
Medicine, Zagazig University
maha18770@gmail.com

References

- Bradley EL. Aclinically based classification system for acute pancreatitis. Summary of the international symposium on acute pancreatitis. *Arch Surg* 1993;128(5):586-590.
- Steinberg W and Tenner S. Acute pancreatitis. *N Engl J Med* 1994;330(17):1198-1210.
- Ates F, Hacievliyagil SS and Karıncaoglu M. Clinical significance of pulmonary function tests in patients with acute pancreatitis. *Digestive Dis and Sci* 2006; 51: 7-10.
- Yamagiwa T, Shimosegawa T, Satoh A, Kimura K, Sakai Y and Masamune A. Inosinealleviate rat caerulein pancreatitis and pancreatitis-associated lung injury. *J Gastroenterol* 2004; 39:41-49.
- Hirota M, Sugita H, Maeda K, Ichibara A and Ogawa M. Concept of SIRS and severe acute pancreatitis. *Nihon Rinsho* 2004; 62(11): 2128-2136.
- Renzulli P, Jakob SM, Täuber M, Candinas D and Gloor B. Severe acute pancreatitis: Case-oriented discussion of interdisciplinary management. *Ancreatology* 2005; 5(3):145-156.
- Browne GW and Pitchumon CS. Pathophysiology of pulmonary complications of acute pancreatitis. *World J Gastroenterol* 2006; 12(44): 7087-7096.
- Mooren FC, Hlouschek V, Finkes T, Turi S, Weber IA, Singh J, Domschke W, Schnekenburger J, Krüger B and Lerch MM. Early changes in pancreatic acinar cell calcium signaling after pancreatic duct obstruction. *J Biological Chemistry* 2003; 278(11): 9361-9369.
- DiMagno MJ and DiMagno EP. New advances in acute pancreatitis. *Curr Opin Gastroenterol* 2007; 23(5): 494-501.
- Schneider A, Lohr J and Singer MV. New international classification of chronic pancreatitis. *Eksp Klin Gastroenterol* 2010; 8:3-16.
- Siu YP, Leung KT, Tong MK and Kwan TH. Use of allopurinol in slowing the progression of renal disease through its ability to lower serum uric acid level. *Am J Kidney Dis* 2005; 47:51-59.
- Isik AT, Mass MR, Yamanel L, Aydin S, Comert B, Akay C, Erdem G and Mas N. The role of allopurinol in experimental acute necrotizing pancreatitis. *Indian J Med Res* 2006;124: 709-714.
- Dowling DK and Simmons LW. Reactive oxygen species as universal constraints in life history evolution. *Proceeding Royal Society B* 2009; 276: 1737-1745.
- Stockert AL and Stechschulte M. Allopurinol to febusostat: How far have we come? *Clim Med Insights: Therapeutics* 2010;2:927-945.
- Kishi S, Takeyama Y, Ueda T, Yasuda T, Shinzeki M, Kuroda Y and Yokozaki H. Pancreatic duct obstruction itself induces expression of α smooth muscle actin in pancreatic stellate cells. *J Surgical Res* 2003; 114: 6-14.
- Bancroft J. and Gamble A. *Theory and Practice of Histology Techniques*. 6th ed., Pp: 83-92, Churchill Livingstone, New York and London, 2008.
- Ramasamy K, Dwyer-Nield LD, Serkova NJ, Hasebroock KM, Tyagi A, Raina K, Singh RP, Malkinson AM and Agarwa IR. Silibinin prevents lung tumorigenesis in wild type but not in iNOS mice: Potential of real time micro CT lung cancer chemoprevention studies. *Clin Cancer Res* 2011; 17: 753-761.
- Singh D. *Principle and Techniques*. In *Histology, Microscopy and Photography*. 1st ed., Pp: 679-699, CBS Publishers and Distributors. New Delhy, Bangalore (India), 2003.
- Bellows CF and Brain JD. Role of fibronectin in pancreatitis-associated lung injury. *Digestive Dis and Sci* 2003; 48(8): 1445-1452.
- Zhang XP, Zhang L, Chen LJ, Chenq QH, Wang JM, Cai W and Cai J. Influence of dexamethasone on inflammatory mediators and NF-kappaB expression in multiple organs of rats with severe acute pancreatitis. *World J Gastroenterology* 2007; 13(4): 548-556.
- Kan SH, Huang F, Tang J, Gao Y and Yuu CL. Role of intrapulmonary expression of inducible Nitric Oxide Synthase gene and nuclear factor κ B activation in severe pancreatitis-associated lung injury. *Inflammation* 2010; 33(5): 287-294.
- Pezzilli R, Bellacosa L and Felicani C. Lung injury in acute pancreatitis. *J Pancreas* 2009; 10(5):481-484.
- Bhatia M, Sidhapuriwala JN, Sparatore A and Moore PK. Treatment with H2S releasing diclofenac protect mice against acute pancreatitis associated lung injury. *Shock* 2008;29(1): 84-88.
- Frossard JL, Saluja A, Bhagat L, Lee HS, Bhatia M, Hofbauer B and Steer ML. The role of intercellular adhesion molecule 1 and neutrophils in acute pancreatitis and pancreatitis-associated lung injury. *Gastroenterology* 1999; 116(3):694-701.
- Lundberg AH, Fukatsu K, Gaber L, Callicutt S, Kotb M, Wilcox H, Kudsk K and Gaber AO. Blocking pulmonary ICAM-1 expression ameliorates lung injury in established diet-induced pancreatitis. *Ann Surg* 2001; 233(2): 213-220.
- Gultekin FA, Kerem M, Tatlicioglu E, Ariciglu A, Unsal C and Bukan N. Leptin treatment ameliorates acute lung injury in rats with cerulean induced acute pancreatitis. *World J Gastroenterology* 2007; 13(21): 2932-2938.
- Al Mofleh IA. Severe acute pancreatitis: Pathogenetic aspects and prognostic factors. *World J Gastroenterol* 2008; 14: 675-684.

28. Raraty MG, Connor S, Criddle DN, Sutton R and Neoptolemos JP. Acute pancreatitis and organ failure: Pathophysiology, natural history and management strategies. *Curr Gastroenterol Rep* 2004; 6:99-103.
29. Pandol SJ, Saluja AK, Imrie CW and Banks PA. Acute pancreatitis: Bench to the bedside. *Gastroentrol* 2007; 132(3): 1127-1151.
30. Alerifi SA, Mubarak M and Alokail MS. Ultrastructure of the pulmonary alveolar cells of rats exposed to Arabian Mix Incense (Ma'amoul). *J Biological Sciences* 2004; 4(6): 694-699.
31. ChvanovM, Petersen OH and Tepikin A. Free radicals and the pancreatic acinar cells: Role in physiology and pathology. *Philos Trans R Soc Lond B Biol Sci* 2005; 360: 2273-2284.
32. Chen YP, Ning JW and Ji F. Establishment of the critical period of sever acute pancreatitis associated lung injury. *Hepatobiliary Pancreat Dis Int* 2009; 8(5): 535-540.
33. Zhang X, Wu D and Jiang X. ICAM-1 and acute pancreatitis complicated by acute lung injury. *J Pancreas* 2009; 10: 8-14.
34. Masubuchi T, Koyama S, Sato E, Takamizawa A, Kubo K, Sekiguchi M, Nagai S and Izumi T. Smoke extract stimulates lung epithelial cells to release neutrophil and monocyte chemotactic activity. *Am J Pathology* 1999; 153(6):1903-1912.
35. Durmus Altun G, Altun A, Aktas RG, Salihoglu YS and Yigitbasi NO. Use of iodine-123 metaiodobenzylguanidine scintigraphy for the detection of amiodarone induced pulmonary toxicity in a rabbit model: A comparative study with technetium-99 m diethyltriaminepenta acetic acid radioaerosolscintigraphy. *Ann Nucl Med* 2005; 19:217-224.
36. Ferguson KK, Loch-Carusio R and Meeker D. Urinary phthalate metabolites in relation to biomarkers of inflammation and oxidative stress: NHANES 1999-2006. *Environ Res* 2011;111(5): 718-726.
37. Akbarshahi H, Rosendahl AH, Westergren-Thorsson G and Andersson R. Acute lung injury in acute pancreatitis- Awaiting the big leap. *Respir Med* 2012; 106(9): 1199-1210.
38. Sato E, Koyama S, Takamizawa A, Masubuchi T, Kubo K, Robbins RA, Nagai S and Izumi T. Smoke extract stimulates lung fibroblasts to release neutrophil and monocytes chemotactic activities. *Am J Physiol* 1999; 227: 1149- 1157.
39. Takamizawa A, Koyama S, Sato E, Masubuchi T, Kubo K, Sekiguchi M, Nagai S and Izumi T. Bleomycin stimulates lung fibroblasts to release neutrophil and monocyte chemotactic activity. *J Immunology* 1999; 162: 6200-6208.
40. Puneet P, Mochhala S and Bhatia M. Chemokines in acute respiratory distress syndrome. *Am J Physiol Lung Cell Mol Physiol* 2005; 288: 3-15.
41. ClosaD, Sabater L, Fernandez-Cruz L, Prats N, Gelpi E and Rosello-Catafau J. Activation of alveolar macrophages in lung injury associated with experimental acute pancreatitis is mediated by the liver. *Ann Surg*1999; 229(2): 230-236.
42. Yuan YZ, Gong ZH, Lou KX, Tu SP, Zhai ZK and YU JU. Involvement of apoptosis of alveolar epithelial cells in acute pancreatitis associated lung injury. *World J Gastroenterology*2000;6(6): 920-924.
43. Gea-Sorli S, Guillamat R, Serrano-Mollar A, Closa D. Activation of lung macrophage subpopulations in experimental acute pancreatitis. *J Pathol* 2011;223(3):417- 424.
44. Schroeder RA, Ewing CA, Sitzmann JV and Kuo PC. Pulmonary expression of iNOS and HO-1 protein upregulated in a rat model of prehepatic portal hypertension. *Dig Dis Sci* 2000; 45: 2405-2410.
45. Maestrelli P, Paska C, Saetta M, Turato G, Nowicki Y, Monti S, Formichi B, Miniati M and Fabbri LM. Decrease haem oxygenase-1 and increased inducible nitric oxide synthase in lung of sever COPD patients. *Eur Respir J* 2003; 21: 971-976.
46. FolchE, Gelpi E, Rosello-catafau J and Closa D. Free radicals generated by xanthine oxidase mediated pancreatitis associated organ failure. *Dig Dis and Sci*1998; 43(11): 2405-2410.
47. Pacher P, Nivorozhkin A and Szabo C. Therapeutic effects of xanthine oxidase inhibitors: Renaissance half a century after the discovery of allopurinol. *Pharmacol Rev* 2006; 58:87-114.
48. Pereda J, Sabater L, Cassinello N, Go'mez-Cambronero L, Closa D, Folch-Puy E, Aparisi L, Calvete J, Cerda M, Liedo S, Vina J and Sastre J. Effect of simultaneous inhibition of TNF-alpha production and xanthine oxidase in experimental acute pancreatitis: The role of mitogen activated protein kinases. *Ann Surg* 2004; 240:108-116.
49. Farghaly EF. Histological study of the protective effect of N-acetylcysteine on pancreatic acinar cells in experimentally induced acute pancreatitis in male albino rats. *Alex Bulletin Fac Med* 2008; 44(2): 589-598.